INNOVATIVE MECHANICAL ENGINEERING **ISSN 2812-9229 (Online)**
University of Niš, Faculty of Mechanical Engineering
VOL. 2, NO 1, 2023, PP. 23 - 42

Original scientific paper *

VIBRATIONS OF FLUID-CONVEYING FUNCTIONALLY GRADED NANOTUBES BASED ON THE REFINED BEAM THEORY IN VARYING TEMPERATURE CONDITIONS

Nikola Despenić, Goran Janevski

University of Niš, Faculty of Mechanical Engineering, Serbia

Abstract. *This paper investigates a model of a fluid-conveying functionally graded (FG) nanotube, based on the refined beam theory in the framework of the nonlocal strain gradient theory. Material properties change smoothly in the radial direction of the nanotube, based on the power-law distribution. Equations of motion are obtained by using Hamilton's principle, while eigenvalues are obtained through Galerkin's method. The influence of the temperature change was noticeable. Two types of temperature changes were considered, uniform and linear temperature rise. The paper deals with the effect of the presence of fluid in the nanotube, which is being conveyed through the nanotube and the effect of the temperature change on the change of natural frequency. Also, the critical fluid velocity and critical thermal buckling load are considered. The influence of the nonlocal and strain gradient parameter on the natural frequency, critical fluid velocity and thermal load should not be neglected. Finally, as mentioned above, the material of the nanotube model depends on the power-law distribution, so the effect of the power-law exponent on the natural frequency and critical fluid velocity is observed.*

Key words: *Nanotube, Fluid conveying, Vibrations, Critical fluid velocity, Functionally graded materials, Thermal buckling*

1. INTRODUCTION

At the end of the 20th century, a group of Japanese researchers invented a novel class of composite materials, called functionally graded materials (FGM). FGM is a type of composite material, whose anisotropic properties can vary. It is already well known that there are FGM structures where the material varies along with the thickness of structures, then axially functionally graded materials, where material varies in the axial direction, as well as bi-directional and three-directional FGM, where the material varies in two or three directions, respectively. The method of production of this type of material, based on powder metallurgy, is given in Zhu et al. [1]. The authors investigated the process of

*Received: December 05, 2022 / Accepted May 23, 2023.
Corresponding author: Nikola Despenić
Faculty of Mechanical Engineering, University of Niš, Serbia
E-mail: nikola.despenic@masfak.ni.ac.rs

preforming and sintering of mixed powders with different compositions and found a suitable fabrication procedure for FGM. They also provided a cross-sectional microscopic view of Z_rO_2 -NiCr fabrication. Mishina et al. [2] investigated the fabrication procedure for joint prostheses, based on the FGM material platform. They also analyzed mechanical properties through fracture toughness, bending strength and wear resistance with different percentages of material in the mixture. The main characteristic of FGM (with pure ceramic and metal ends) is that material properties (Young's modulus, density, Poisson's ratio etc.) change smoothly through the nanostructure. Kurimoto et al. [3] investigated potential application of FGM with dielectric permittivity for reducing electric field stress on the electrode surface. Also, investigation of this type of FGM fabrication was considered. Kato et al. [4] obtained results for FGM applications as a solid insulator (spacer) for a gaseous insulation system.

NEMS and MEMS and their mechanical behavior have been of interest in the past, and there are numerous papers on this topic in the literature. It is well known that the classical continuum theory cannot be applied to small structures. Based on the need for a theory which can be acceptable for mathematical modeling of small structures, Eringen [5, 6] developed a theory which includes size-dependent effects. The difference between these theories is based on the fact that the stress at a reference point depends on the strain in the region near that point. In the framework of Eringen's theory, Eltaher et al. [7] investigated the bending and buckling behavior of an FGM Euler-Bernoulli nanobeam model. Maximum deflection and critical buckling load with a different power-law exponent and nonlocal parameter were found using the Galerkin finite element method. Also, Eltaher et al [8] considered vibrations of an FGM Euler-Bernoulli nanobeam model, using finite element method. Ebrahimi and Salari [9] analyzed various types of thermal loading and their impact on the vibration of a simply supported FGM nanobeam, where material vary in the thickness direction, in a power-law FG form. Natural frequencies and thermal buckling loading were obtained by using the semi analytical method, called differential transform method (DTM). They also considered two different types of thermal load, linear and nonlinear. The impact of thermal load on the natural frequencies of a Timoshenko FG nanobeam model was investigated by Ebrahimi and Salari [10]. The solutions were obtained through the Navier solution method. Critical buckling load was obtained for different values of thickness, nonlocal parameter, and gradient index. The impact of thermal load on the dimensionless natural frequency was also observed. Based on Eringen's nonlocal theory, Jouneghani et al. [11] investigated the bending behavior of a FG porous nanobeam under a hygro-thermo-mechanical influence. The effect of the material length-scale, power-law exponent, porosity volume fraction, thermal load and moisture concentration on the bending of the nanobeam were considered. Vibrations of viscoelastic FG nanobeams with hygro-thermal influence were also considered by Ebrahimi and Barati [12]. A mathematical model of an FG nanobeam was obtained by using a higher order refined beam theory in the framework of the nonlocal strain gradient theory. The problem discussed in this paper was based on the FG nanobeam model resting on a viscoelastic Winkler-Pasternak foundation with an impact on the thermal load, damping coefficient, Winkler and Pasternak coefficient, gradient index, etc. Using the nonlocal strain gradient theory, Şimşek [13] obtained analytical solutions for static deflection, buckling, free and forced vibration of FG nanobeams. Dimensionless deflection, critical buckling load, dimensionless natural frequency of free and forced vibrations were obtained. The impact of the nonlocal and strain gradient

parameter, and the gradient index on statics, stability and vibrations were considered. The author considered two different types of forced vibration, under stationary harmonic load and under moving load, and illustrated how dynamic amplification factor was changed through the dimensionless time. Lim et al. [14] established a higher-order nonlocal strain gradient theory, which was considered in many papers in the literature. Janevski et al. [15] investigated the impact of the higher order strain gradient nonlocal parameters and length-scale parameter on the thermal buckling and vibrations of an FG Euler-Bernoulli nanobeam model. Dimensionless buckling temperature load and nondimensional natural frequency were examined for different types of temperature change, power-law exponent and different values of the length and thickness ratio. Vibrations of Timoshenko FG nanobeams in varying temperature conditions, based on the higher order strain gradient theory were considered by Janevski et al. [16]. When it comes to the higher order strain gradient theory, Nematollahi and Mohammadi [17] considered vibration analysis of a simply supported sandwich nanoplate and illustrated the amplitude and frequency change due to the change in nonlocal parameters.

Static and dynamic behavior of nanotubes has been previously observed. The scientific community has grown interested in topics with buckling analysis, vibrations, wave propagation etc. She et al. [18] investigated critical buckling thermal load of a functionally graded simply supported and clamped nanotube model, using the refined beam theory, for different nonlocal parameters, nanotube dimensions, porosity volume fractions, etc. Vibrations of a simply supported porous nanotube, with thermal load, based on nonlocal strain gradient theory were considered by She et al. [19]. Through the Navier solution method, dimensionless natural frequency was obtained with influence of thermal load, porosity effect, nonlocal and strain gradient parameter. The impact of the volume fraction index and the porosity volume fraction on nondimensional natural frequency was calculated, for the first four modes. She et al. [20] considered the porous nanotube's wave propagation and the impact of the nonlocal parameter and length-scale parameter on the dispersion relation at high and low wave numbers used in the nonlocal strain gradient theory. Shafiei and She [21] considered vibrations of two directional functionally graded nanotubes with existing thermal load. The generalized differential quadrature method was employed to solve the equations. Buckling and post-buckling characteristics of FG microtubes with initial geometric imperfection were considered in the paper by Lu et al. [22]. A couple of typical distribution patterns of composite materials and von-Kármán's geometric nonlinearity were used for the post-buckling investigation. Karami and Janghorban [23] studied free vibrations of porous nanotubes, based on the Timoshenko beam model, and considered the effect of varying thickness and power-law exponent on nondimensional frequency.

The scientific community has hugely contributed to the investigation of fluid-structure interaction (FSI). FSI represents how the presence of fluid affects various structural analysis, including vibration, fatigue, damage, stress analysis, buckling analysis etc. When it comes to nanofluids and nanostructures, the impact of nonlocal parameters, besides the fluid impact, has also been found interesting. Wang [24] obtained an analytical solution of a fluid-conveying nanotube with the surface layer effect, by integrating the nonlocal elasticity model with the surface elasticity model. In this paper, the influence of the dimensionless fluid velocity on the dimensionless natural frequency was illustrated. Also, the impact of tube thickness on the dimensionless critical flow velocity was calculated. Based on the above, stability analysis is very important.

Seyranian and Mailybaev [25] analyzed stability boundaries for different problems, including fluid flow through an elastic simply supported tube. Based on the nonlocal elasticity theory, Deng et al. [26] considered the effect of fluid-conveying through the multi-span viscoelastic FG nanotube model. The equation was obtained by using a hybrid method, and the impact of fluid velocity, power-law exponent, nonlocal parameter and internal damping on dimensionless natural frequency and stability were considered. Also, the variation of the volume fraction exponent and dimensionless nonlocal parameter and their impact on the dimensionless critical fluid velocity was illustrated. Liu et al. [27] investigated nonlinear vibration and stability analysis of an FG nanotube model with a geometrical initial imperfection of the nanotube in the framework of the nonlocal strain gradient theory. They also included the geometrical von-Kármán nonlinearity. They observed a decrease in the dimensionless natural frequency with an increase in the dimensionless fluid velocity. The impact of the power-law exponent and oscillation amplitude on the dimensionless fluid velocity for different values of the initial imperfection amplitude was also illustrated. Nonlinear analysis of fluid-conveying nanotubes based on the nonlocal strain gradient theory was considered in the paper by Farajpour et al. [28]. The impact of different solid and fluid parameters and flow speed on the nonlinear resonance were considered. Influence of the residual surface stress on the dynamical behavior of double-walled nanotubes was considered by Hosseini and Ghadiri [29]. The bifurcation of a fluid-conveying double-walled nanotube model with geometrical von-Kármán nonlinearity was considered with the surface effect and nonlocal elasticity. The approach used for solving equations was the Galerkin method with the multiple scale method. Bahaadini and Hosseini [30] investigated the stability analysis of the fluid-conveying carbon nanotube subjected to a magnetic field and resting on a Winkler and Pasternak foundation. The partial differential equations were described by the Hamiltonian principle and obtained by using the extended Galerkin approach for different boundary conditions. Based on the Timoshenko beam theory, Ghane et al. [31] analyzed vibrations of fluid-conveying nanotubes with the impact of a magnetic field. The considered nanotube model was thin-walled, and equations were obtained through Hamilton's principle and the nonlocal strain gradient theory. The influence of the nonlocal parameter, strain gradient length scale, magnetic nanoflow, and Knudsen number on the natural frequency and critical fluid velocity were considered. Nematollahi et al. [32] identified and predicted the fluid velocity and mass ratio of a piezoelectric nanotube model with fluid conveying through it by using the Levenberg-Marquardt and artificial neural network methods. The governing equations of motion for the Euler-Bernoulli beam with the combination of Eringen's nonlocal elasticity theory were used to obtain natural frequencies of the mentioned model with the Galerkin method.

This paper investigates a fluid-conveying FG nanotube model based on the nonlocal strain gradient theory and higher order refined beam theory. The material properties are smoothly changed along with the thickness of the nanotube, with respect to the power-law mixture rule. The equations of motion will be obtained using Hamilton's principle, and natural frequencies and other characteristics of this considered problem will be calculated by using Galerkin's method. Nondimensional natural frequencies of the nanotube without the effect of fluid conveying will be compared with the reference paper She et al. [19]. Natural frequencies, with and without the fluid effect, will be obtained and presented for three different beam theories, namely, the Euler-Bernoulli, Timoshenko and higher order refined beam theory. The dimensionless critical fluid velocity and the

impact of the dimensionless fluid velocity on the nondimensional natural frequency will be obtained and illustrated. Through the analysis of the critical fluid velocity and natural frequency, the impact of the nonlocal and length-scale parameter will be considered. Also, the effect of the thermal load will be explained. Two different types of thermal load, uniform and linear, will be discussed in this paper. Critical thermal load and impact of the thermal load on the nondimensional natural frequencies will be obtained, presented and illustrated.

2. MATHEMATICAL MODEL

2.1 The nonlocal strain gradient theory for the FG nanotube model

The classical continuum theories have certain limitations for application to nanostructures. Based on that fact, in a group of theories that were suggested in the past for this type of structure, one could also find the nonlocal strain gradient theory. The constitutive relations of the nonlocal strain gradient theory can be written as

$$\left(1-\left(ea\right)^2\nabla^2\right)\boldsymbol{t}_{ij}=\boldsymbol{C}_{ijk}\boldsymbol{\varepsilon}_{ij}-l^2\boldsymbol{C}_{ijk}\nabla^2\boldsymbol{\varepsilon}_{ij}, \tag{1}$$

where C_{ijk} is the elastic modulus tensor of classical elasticity, ε_{ij} is the Cartesian component, while t_{ij} is the nonlocal total strain gradient stress tensor, e is the nonlocal material constant, a is the internal characteristic length, l is the strain gradient length scale parameter and ∇^2 is the Laplacian operator. The total nonlocal strain gradient stress tensor $\boldsymbol{t}_{ij}$ can be expressed as (Lim et al. [14])

$$\boldsymbol{t}_{ij}=\boldsymbol{\sigma}_{ij}-\nabla\boldsymbol{\sigma}_{ij}^{(1)}, \tag{2}$$

in which the classical stress tensor $\boldsymbol{\sigma}_{ij}$ and the higher-order stress tensor $\boldsymbol{\sigma}_{ij}^{(1)}$ can be written as follows

$$\boldsymbol{\sigma}=\int_V\boldsymbol{\alpha}_0\left(\left|x-x'\right|,e_0a\right)\boldsymbol{C}:\boldsymbol{\varepsilon}'dV',\ \boldsymbol{\sigma}^{(1)}=l^2\int_V\boldsymbol{\alpha}_1\left(\left|x-x'\right|,e_0a\right)\boldsymbol{C}:\nabla\boldsymbol{\varepsilon}'dV', \tag{3}$$

where the classical stress tensor and the higher-order stress tensor are the stresses at the point x and at the near point x', $\boldsymbol{C}$ is the fourth-order tensor of classical linear elastic material moduli, while "$:$" is used as a symbol for double-dot product. For an elastic material, considering one dimensional case and based on polar coordinates, the generalized nonlocal constitutive relations in a differential form based on the nonlocal strain gradient theory can be simplified as

$$\left(1-\mu^2\frac{\partial^2}{\partial x^2}\right)t_{xx}=\left(1-l^2\frac{\partial^2}{\partial x^2}\right)E\left(r,T\right)\varepsilon_{xx}, \tag{4}$$

$$\left(1-\mu^2\frac{\partial^2}{\partial x^2}\right)t_{xz}=\left(1-l^2\frac{\partial^2}{\partial x^2}\right)G(r,T)\gamma_{xz}, \tag{5}$$

$$\left(1-\mu^2\frac{\partial^2}{\partial x^2}\right)t_{xy}=\left(1-l^2\frac{\partial^2}{\partial x^2}\right)G(r,T)\gamma_{xy}. \tag{6}$$

where ε_x, γ_{xz} and γ_{xy} are the axial and shear strain, $\mu = ea$ is the nonlocal parameter, E is Young's modulus and $G=\dfrac{E}{2(1+\nu)}$ is the shear modulus.

2.2 Material properties and geometry

Consider a functionally graded nanotube with length L, inner radius R_i and outer radius R_o (Fig. 1). Material properties vary along the radial direction of the nanotube model. According to the rule of mixture [33], the effective material properties P_f can be written as

$$P_f(T,r)=P_c(T)V_c(r)+P_m(T)V_m(r), \tag{7}$$

where $V_c(r)$ is the volume fraction of the ceramic and $V_m(r)$ is the volume fraction of the metal, while P_c and P_m are temperature dependent material properties for ceramic and metal, respectively. Using the power-law distribution, these volume fractions can be expressed as

$$V_c(r)=\left(\frac{r-R_i}{R_o-R_i}\right)^p,\ V_m(r)=1-V_c(r),\ R_i\le r\le R_o. \tag{8}$$

Fig. 1 Geometry and coordinates of FG nanotube model

The material properties in the function of temperature (such as Young's modulus E, thermal expansion coefficient α, mass density ρ, thermal conductivity κ and Poisson's ratio ν) can be written as follows (Touloukian [34])

$$P_{c,m}(T)=P_0\left(P_{-1}T^{-1}+1+P_1T+P_2T^2+P_3T^3\right), \tag{9}$$

where P_0, P_{-1}, P_1, P_2 and P_3 are the coefficients that can be seen in the table of material properties for Si_3N_4 and $SUS304$ (Table 1). For the power-law distribution (2), the effective material properties are

$$P_f(r,T) = \left(P_c(T) - P_m(T)\right)\left(\frac{r-R_i}{R_o-R_i}\right)^p + P_m(T). \tag{10}$$

The inner surface $(r = R_i)$ of the FG nanotube is pure metal $(SUS304)$ and the outer surface $(r = R_o)$ is pure ceramic (Si_3N_4).

Table 1 Temperature-dependent coefficient of Young's modulus E, thermal expansion coefficient α, mass density ρ, thermal conductivity κ and Poisson's ratio ν for Si_3N_4 and $SUS304$

Material	Properties	P_0	P_{-1}	P_1	P_2	P_3
Si_3N_4	$E\ [Pa]$	348.43e+9	0	-3.010e-4	2.160e-7	-8.946e-11
	$\alpha\ \left[K^{-1}\right]$	5.8723e-6	0	9.095ee-4	0	0
	$\rho\ \left[kg/m^3\right]$	2370	0	0	0	0
	ν	0.24	0	0	0	0
$SUS304$	$E\ [Pa]$	201.04e+9	0	3.079e-4	-6.534e-7	0
	$\alpha\ \left[K^{-1}\right]$	12.330e-6	0	8.086e-4	0	0
	$\rho\ \left[kg/m^3\right]$	8166	0	0	0	0
	ν	0.3262	0	-2.002e-4	3.797e-7	0

2.3 Kinematic relations

The displacement field, based on the refined beam theory, of any material point in x, y and z direction can be written based on Zhang-Fu model [35]

$$q_x = u(x,t) - z\frac{\partial w}{\partial x} + g(y,z)\left[\frac{\partial w}{\partial x} + \psi(x,t)\right], \tag{11}$$

$$q_y = 0, \tag{12}$$

$$q_z = w(x,t), \tag{13}$$

where $u(x,t)$ and $w(x,t)$ are the axial and transverse displacement components of the mid-plane in the x and z direction, respectively, $\psi(x,t)$, while function $g(y,z)$ can be expressed as

$$g\left(y,z\right)=z+z\frac{R_1^{\,2}R_0^{\,2}/r^2-r^2/3}{R_1^{\,2}+R_0^{\,2}}. \tag{14}$$

The strain field, based on equations (11), (12) and (13), and in line with the refined beam theory, can be written as

$$\varepsilon_{xx}=\frac{\partial q_x}{\partial x}=\frac{\partial u}{\partial x}-z\frac{\partial^2 w}{\partial x^2}+g\left(y,z\right)\left(\frac{\partial^2 w}{\partial x^2}+\frac{\partial \psi}{\partial x}\right), \tag{15}$$

$$\gamma_{xz}=\frac{\partial q_x}{\partial z}+\frac{\partial q_z}{\partial x}=\frac{\partial g}{\partial z}\left(\frac{\partial w}{\partial x}+\psi\left(x,t\right)\right), \tag{16}$$

$$\gamma_{xy}=\frac{\partial q_x}{\partial y}+\frac{\partial q_y}{\partial x}=\frac{\partial g}{\partial y}\left(\frac{\partial w}{\partial x}+\psi\left(x,t\right)\right). \tag{17}$$

The relationship between the cylindrical $Or\theta x$ coordinate system and the Cartesian $Oxyz$ coordinate system can be expressed as

. $$y=r\cos\theta,\quad z=r\sin\theta,\quad r^2=y^2+z^2,\quad 0\le x\le L. \tag{18}$$

To derive governing equations of motion, Hamilton's principle is used and can be expressed as

$$\int_{t_1}^{t_2}\left(\delta U+\delta V-\delta T_p-\delta T_f\right)dt=0, \tag{19}$$

in which $t_1<t<t_2$. δU is the virtual strain energy

$$\begin{aligned}
\delta U&=\int_V\left[\sigma_{xx}\delta\varepsilon_{xx}+\tau_{xz}\delta\gamma_{xz}+\tau_{xy}\delta\gamma_{xy}+\sigma_{xx}^{(1)}\nabla\delta\varepsilon_{xx}+\tau_{xz}^{(1)}\nabla\delta\gamma_{xz}+\tau_{xy}^{(1)}\nabla\delta\gamma_{xy}\right]dv,\\
\delta U&=\int_0^L\left[N_{xx}\frac{\partial\delta u}{\partial x}-M_{xx}\frac{\partial^2\delta w}{\partial x^2}+P\left(\frac{\partial^2\delta w}{\partial x^2}+\frac{\partial\delta\psi}{\partial x}\right)+Q\left(\frac{\partial\delta w}{\partial x}+\delta\psi\right)\right]dx\\
&\quad+\left[N_{xx}^{(1)}\frac{\partial\delta u}{\partial x}-M_{xx}^{(1)}\frac{\partial^2\delta w}{\partial x^2}+P^{(1)}\left(\frac{\partial^2\delta w}{\partial x^2}+\frac{\partial\delta\psi}{\partial x}\right)+Q^{(1)}\left(\frac{\partial\delta w}{\partial x}+\delta\psi\right)\right]_0^L,
\end{aligned} \tag{20}$$

where the following stress resultants are expressed as

$$\left(N_{xx},\,M_{xx},P\right)=\int_A\left(1,z,g\right)t_{xx}dA,\;\;Q=\int_A\left(t_{xz}\frac{\partial g}{\partial z}+t_{xy}\frac{\partial g}{\partial y}\right)dA, \tag{21}$$

$$\left(N_{xx}^{(1)},\,M_{xx}^{(1)},P^{(1)}\right)=\int_A\left(1,z,g\right)\sigma_{xx}^{(1)}dA,\;\;Q^{(1)}=\int_A\left(\tau_{xz}^{(1)}\frac{\partial g}{\partial z}+\tau_{xy}^{(1)}\frac{\partial g}{\partial y}\right)dA. \tag{22}$$

Virtual kinetic energy of the nanotube model δT_p can be defined in the following form

$$\begin{aligned}\delta T_p &= \frac{1}{2}\int_v \rho(T,r)\delta\left(\left(\frac{\partial q_x}{\partial t}\right)^2+\left(\frac{\partial q_y}{\partial t}\right)^2+\left(\frac{\partial q_z}{\partial t}\right)^2\right)dv = \\ &= \int_0^L\Bigg[I_0\left(\frac{\partial u}{\partial t}\frac{\partial \delta u}{\partial t}+\frac{\partial w}{\partial t}\frac{\partial \delta w}{\partial t}\right)+I_1\frac{\partial^2 w}{\partial x\partial t}\frac{\partial^2 \delta w}{\partial x\partial t} \\ &\quad -I_2\left(\frac{\partial^2 w}{\partial x\partial t}\frac{\partial \delta \psi}{\partial t}+2\frac{\partial^2 w}{\partial x\partial t}\frac{\partial^2 \delta w}{\partial x\partial t}+\frac{\partial \psi}{\partial t}\frac{\partial^2 \delta w}{\partial x\partial t}\right) \\ &\quad +I_3\left(\frac{\partial^2 w}{\partial x\partial t}\frac{\partial^2 \delta w}{\partial x\partial t}+\frac{\partial \psi}{\partial t}\frac{\partial^2 \delta w}{\partial x\partial t}+\frac{\partial^2 w}{\partial x\partial t}\frac{\partial \delta \psi}{\partial t}+\frac{\partial \psi}{\partial t}\frac{\partial \delta \psi}{\partial t}\right)\Bigg]dx,\end{aligned} \tag{23}$$

where the mass moments of inertia are defined as follows

$$(I_0,I_1,I_2,I_3)=\int_{R_0}^{R_1}\int_0^{2\pi}(1,z^2,zg,g^2)\rho(r,T)rdrd\theta. \tag{24}$$

Considering the thermal expansion, the expression of variation of the virtual work δV is as follows

$$\delta V=-\int_v E(T,r)\alpha(T,r)(T-T_0)\frac{\partial w}{\partial x}\frac{\partial}{\partial x}(\delta w)dv=-\int_0^L\left(N^T\frac{\partial w}{\partial x}\frac{\partial}{\partial x}(\delta w)\right)dx, \tag{25}$$

where N^T is the thermal force resultant

$$N^T=\int_{R_0}^{R_1}\int_0^{2\pi}E(T,r)\alpha(T,r)(T-T_0)rdrd\theta, \tag{26}$$

and T_0=300K is the reference temperature. The virtual kinetic energy of the fluid can be written as [24]

$$\begin{aligned}\delta T_f &= \frac{1}{2}\int_v \rho_f\delta\left(\left(\frac{\partial u}{\partial t}+V+V\frac{\partial u}{\partial x}\right)^2+\left(\frac{\partial w}{\partial t}+V\frac{\partial w}{\partial x}\right)^2\right)dv = \\ &= m_f\int_0^L\left(\left(\frac{\partial u}{\partial t}+V+V\frac{\partial u}{\partial x}\right)\left(\frac{\partial \delta u}{\partial t}+V\frac{\partial \delta u}{\partial x}\right)+\left(\frac{\partial w}{\partial t}+V\frac{\partial w}{\partial x}\right)\left(\frac{\partial \delta w}{\partial t}+V\frac{\partial \delta w}{\partial x}\right)\right)dx,\end{aligned} \tag{27}$$

where $m_f=\rho_f A_f$ presents mass of the fluid.

The governing equations of motion can be achieved by substituting Eqs. (20), (23), (25) and (27) into Eq. (19), using integration by parts and setting the coefficients of δu and δw to zero

$$\delta u:\ \frac{\partial N_{xx}}{\partial x}=(I_0+m_f)\frac{\partial^2 u}{\partial t^2}+2m_fV\frac{\partial^2 u}{\partial x\partial t}+m_fV^2\frac{\partial^2 u}{\partial x^2}, \tag{28}$$

$$\delta\psi\text{:}\ \frac{\partial P}{\partial x}-Q=-I_2\frac{\partial^3 w}{\partial x\partial t^2}+I_3\left(\frac{\partial^3 w}{\partial x\partial t^2}+\frac{\partial^2\psi}{\partial t^2}\right), \tag{29}$$

$$\begin{aligned}\delta w\text{:}\ \frac{\partial^2 M_{xx}}{\partial x^2}-\frac{\partial^2 P}{\partial x^2}+\frac{\partial Q}{\partial x}&=\left(I_0+m_f\right)\frac{\partial^2 w}{\partial t^2}-I_1\frac{\partial^4 w}{\partial x^2\partial t^2}\\&+I_2\left(2\frac{\partial^4 w}{\partial x^2\partial t^2}+\frac{\partial^3\psi}{\partial x\partial t^2}\right)-I_3\left(\frac{\partial^4 w}{\partial x^2\partial t^2}+\frac{\partial^3\psi}{\partial x\partial t^2}\right)\\&+2m_f V\frac{\partial^2 w}{\partial x\partial t}+m_f V^2\frac{\partial^2 w}{\partial x^2}+N^T\frac{\partial^2 w}{\partial x^2},\end{aligned} \tag{30}$$

with appropriate classical boundary conditions

$$N_{xx}-m_f\left(V\frac{\partial u}{\partial t}+V^2+V^2\frac{\partial u}{\partial x}\right)=0\quad\text{or}\quad u=0, \tag{31}$$

$$P-M_{xx}=0\quad\text{or}\quad\frac{\partial w}{\partial x}=0, \tag{32}$$

$$\begin{aligned}&\frac{\partial M_{xx}}{\partial x}-\frac{\partial P}{\partial x}+Q-\left(I_1-2I_2+I_3\right)\frac{\partial^3 w}{\partial x\partial t^2}-\left(I_3-I_2\right)\frac{\partial^2\psi}{\partial t^2}\\&-m_f\left(V\frac{\partial w}{\partial t}+V^2\frac{\partial w}{\partial x}\right)-N^T\frac{\partial w}{\partial x}=0,\quad\text{or}\quad w=0,\end{aligned} \tag{33}$$

$$P=0\quad\text{or}\quad\psi=0. \tag{34}$$

Based on Eqs. (4-6), after integrating both sides and after some manipulations, the stress resultants can be defined as

$$N_{xx}=\mu^2\frac{\partial^2 N_{xx}}{\partial x^2}+\left(1-l^2\frac{\partial^2}{\partial x^2}\right)A_{xx}\frac{\partial u}{\partial x}, \tag{35}$$

$$M_{xx}=\mu^2\frac{\partial^2 M_{xx}}{\partial x^2}+\left(1-l^2\frac{\partial^2}{\partial x^2}\right)\left[-B_{xx}\frac{\partial^2 w}{\partial x^2}+D_{xx}\left(\frac{\partial^2 w}{\partial x^2}+\frac{\partial\psi}{\partial x}\right)\right], \tag{36}$$

$$P=\mu^2\frac{\partial^2 P}{\partial x^2}+\left(1-l^2\frac{\partial^2}{\partial x^2}\right)\left[-D_{xx}\frac{\partial^2 w}{\partial x^2}+E_{xx}\left(\frac{\partial^2 w}{\partial x^2}+\frac{\partial\psi}{\partial x}\right)\right], \tag{37}$$

$$Q=\mu^2\frac{\partial^2 Q}{\partial x^2}+\left(1-l^2\frac{\partial^2}{\partial x^2}\right)C_{yz}\left(\frac{\partial w}{\partial x}+\psi\right), \tag{38}$$

in which the cross-sectional rigidities are

$$\begin{aligned}&\left(A_{xx},B_{xx},D_{xx},E_{xx}\right)=\int_{R_0}^{R_1}\int_{0}^{2\pi}\left(1,z^2,zg,g^2\right)E\left(r,T\right)rdrd\theta,\\&C_{yz}=\int_{R_0}^{R_1}\int_{0}^{2\pi}G\left(r,T\right)\left(\frac{\partial^2 g}{\partial z^2}+\frac{\partial^2 g}{\partial y^2}\right)rdrd\theta.\end{aligned}\tag{39}$$

The nonlocal governing equations of motion of the FG nanotube model can be derived after substituting the derivative of N_{xx}, M_{xx}, P, and Q into Eqs. (28-30), so the equations can be expressed as

$$\begin{aligned}&\left(1-l^2\frac{\partial^2}{\partial x^2}\right)A_{xx}\frac{\partial^2 u}{\partial x^2}=\\&=\left(1-\mu^2\frac{\partial^2}{\partial x^2}\right)\left[\left(I_0+m_f\right)\frac{\partial^2 u}{\partial t^2}-I_1\frac{\partial^3 w}{\partial x\partial t^2}+2m_fV\frac{\partial^2 u}{\partial x\partial t}+m_fV^2\frac{\partial^2 u}{\partial x^2}\right],\end{aligned}\tag{40}$$

$$\begin{aligned}&\left(1-l^2\frac{\partial^2}{\partial x^2}\right)\left[-D_{xx}\frac{\partial^3 w}{\partial x^3}+E_{xx}\left(\frac{\partial^3 w}{\partial x^3}+\frac{\partial^2\psi}{\partial x^2}\right)-C_{yz}\left(\frac{\partial w}{\partial x}+\psi\right)\right]=\\&=\left(1-\mu^2\frac{\partial^2}{\partial x^2}\right)\left[-I_2\frac{\partial^3 w}{\partial x\partial t^2}+I_3\left(\frac{\partial^3 w}{\partial x\partial t^2}+\frac{\partial^2\psi}{\partial t^2}\right)\right],\end{aligned}\tag{41}$$

$$\begin{aligned}&\left(1-l^2\frac{\partial^2}{\partial x^2}\right)\left[-B_{xx}\frac{\partial^4 w}{\partial x^4}+D_{xx}\left(\frac{\partial^4 w}{\partial x^4}+\frac{\partial^3\psi}{\partial x^3}\right)+D_{xx}\frac{\partial^4 w}{\partial x^4}\right.\\&\left.-E_{xx}\left(\frac{\partial^4 w}{\partial x^4}+\frac{\partial^3\psi}{\partial x^3}\right)+C_{yz}\left(\frac{\partial^2 w}{\partial x^2}+\frac{\partial\psi}{\partial x}\right)\right]=\\&=\left(1-\mu^2\frac{\partial^2}{\partial x^2}\right)\left[\left(I_0+m_f\right)\frac{\partial^2 w}{\partial t^2}-I_1\frac{\partial^4 w}{\partial x^2\partial t^2}+I_2\left(2\frac{\partial^4 w}{\partial x^2\partial t^2}+\frac{\partial^3\psi}{\partial x\partial t^2}\right)\right.\\&\left.-I_3\left(\frac{\partial^4 w}{\partial x^2\partial t^2}+\frac{\partial^3\psi}{\partial x\partial t^2}\right)+2m_fV\frac{\partial^2 w}{\partial x\partial t}+m_fV^2\frac{\partial^2 w}{\partial x^2}+N^T\frac{\partial^2 w}{\partial x^2}\right].\end{aligned}\tag{42}$$

In the present work, the results of natural frequencies and critical buckling load are presented for the case of uniform temperature rise (UTR) and linear temperature rise (LTR). The temperature of the FG nanotube uniformly rises by ΔT [17]

$$T\left(r\right)=T_0+\Delta T=const.\tag{43}$$

In the case of a linear temperature rise (LTR), and based on the reference where LTR is introduced for the beam model [7], the temperature of the FG nanotube varies linearly along the radius of the nanotube

$$T\left(r\right)=T_m+\Delta T\left(\frac{r-R_0}{R_1-R_0}\right),\tag{44}$$

Where $T_c=T(R_1)$ and $T_m=T(R_0)$ are the temperatures of the inner and the outer surface of the nanotube respectively, while $\Delta T=T_c-T_m$. In this paper, it is assumed that the temperature of the bottom surface is $T_m=T_0+5=305$K.

3. SOLUTION PROCEDURES

It must be noticed that Eq. (40) is totally independent. After neglecting the Eq. (40), calculating the remaining two Eqs. (41,42) can be started with assuming the solution in the shape that satisfies the corresponding boundary conditions (31-34)

$$\psi(x,t)=\sum_{k=1}^{N}\Psi_k\cos(\lambda x)e^{i\omega_k t}=\sum_{k=1}^{N}\Psi_k\eta_k(x)e^{i\omega_k t} \tag{45}$$

$$w(x,t)=\sum_{k=1}^{N}W_k\sin(\lambda x)e^{i\omega_k t}=\sum_{k=1}^{N}W_k\varphi_k(x)e^{i\omega_k t} \tag{46}$$

where $\lambda=k\pi/L$ and Ψ_k, W_k are the unknown coefficients. Applying Galerkin's method and substituting the solutions into Eqs. (41,42), one gets

$$\left(\begin{bmatrix}K_{11} & K_{12}\\ K_{21} & K_{22}\end{bmatrix}-\omega_k{}^2\begin{bmatrix}M_{11} & M_{12}\\ M_{21} & M_{22}\end{bmatrix}\right)\begin{pmatrix}\Psi_k\\ W_k\end{pmatrix}=0, \tag{47}$$

where $\left[K_{ij}\right]$ and $\left[M_{ij}\right]$ are the stiffness and mass matrices, respectively. The coefficients in the stiffness matrix are

$$\begin{aligned}
K_{11}&=E_{xx}\left(k_{12}-l^2k_{14}\right)-C_{yz}\left(k_{10}-l^2k_{12}\right),\\
K_{12}&=\left(E_{xx}-D_{xx}\right)\left(s_{13}-l^2s_{15}\right)-C_{yz}\left(s_{11}-l^2s_{13}\right),\\
K_{21}&=-\left(E_{xx}-D_{xx}\right)\left(p_{13}-l^2p_{15}\right)+C_{yz}\left(p_{11}-l^2p_{13}\right),\\
K_{22}&=\left(2D_{xx}-B_{xx}-E_{xx}\right)\left(c_{14}-l^2c_{16}\right)+C_{yz}\left(c_{12}-l^2c_{14}\right)\\
&-\left(m_fV^2+N^T\right)\left(c_{12}-\mu^2c_{14}\right),
\end{aligned} \tag{48}$$

and the coefficients in the mass matrix

$$\begin{aligned}
M_{11}&=-I_3\left(k_{10}-\mu^2k_{12}\right),\\
M_{12}&=\left(I_2-I_3\right)\left(s_{11}-\mu^2s_{13}\right),\\
M_{21}&=\left(I_3-I_2\right)\left(p_{11}-\mu^2p_{13}\right),\\
M_{22}&=-\left(I_0+m_f\right)\left(c_{10}-\mu^2c_{12}\right)-\left(2I_2-I_1-I_3\right)\left(c_{12}-\mu^2c_{14}\right),
\end{aligned} \tag{49}$$

in which

$$
\begin{aligned}
&k_{10}=\int_0^L \eta_k\eta_k dx, \quad k_{12}=\int_0^L \eta_k''\eta_k dx, \quad k_{14}=\int_0^L \eta_k^{(IV)}\eta_k dx,\\
&s_{11}=\int_0^L \varphi_k'\eta_k dx, \quad s_{13}=\int_0^L \varphi_k'''\eta_k dx, \quad s_{15}=\int_0^L \varphi_k^{(V)}\eta_k dx,\\
&p_{11}=\int_0^L \varphi_k\eta_k' dx, \quad p_{13}=\int_0^L \varphi_k\eta_k''' dx, \quad p_{15}=\int_0^L \varphi_k\eta_k^{(V)} dx,\\
&c_{10}=\int_0^L \varphi_k\varphi_k dx, \quad c_{11}=\int_0^L \varphi_k'\varphi_k dx, \quad c_{12}=\int_0^L \varphi_k''\varphi_k dx,\\
&c_{13}=\int_0^L \varphi_k'''\varphi_k dx, \quad c_{14}=\int_0^L \varphi_k^{(IV)}\varphi_k dx, \quad c_{16}=\int_0^L \varphi_k^{(VI)}\varphi_k dx
\end{aligned}
\tag{50}
$$

4. RESULTS AND DISCUSSION

In this part, an overview and analysis of the results are given. Impact of fluid conveying, thermal load, nonlocal parameter and power-law exponent on the natural frequency was investigated. Also, critical fluid velocity and critical buckling thermal load were part of this investigation. Geometry of the nanotube model is presented in Fig. 1, with the following dimensions: inner radius R_I=0.5nm and outer radius R_O=1nm. The results are presented for two cases of nanotube length, L=20nm and L=100nm. Functionally graded nanotube is composed of metal (SUS304) for the inner surface and ceramic (Si_3N_4) for the outer surface.

As mentioned above, the inspiration for this investigation was found in [17], so the comparison of the presented method is confirmed for the same parameters. For different values of the nonlocal parameter μ and the strain gradient length scale parameter l, the results are presented in the Table (2,3). For this purpose, the dimensionless velocity $v=V\sqrt{m_f L^2/E_{m0}I_f}$, that is introduced by Liu et al. [24], is set to zero. Also, the values such as $\Delta T=0$, $p=1$, $R_i/R_o=0.5$, $L/R_o=20$ and $\Omega_k=\omega_k\left(L^2/R_1\right)\sqrt{\rho_{m0}/E_{m0}}$ are used for this comparison.

Table 2 Comparisons of the nondimensional natural frequency for SS FG nanotube with various values of the nonlocal parameter μ and using UTR

$\mu\ (nm)$		Ω_1	Ω_2	Ω_3
0	She et al. [17]	8.234	31.154	64.833
	Present	8.2346	31.1597	64.8547
1	She et al. [17]	8.134	29.722	58.647
	Present	8.1349	29.7272	58.6670
2	She et al. [17]	7.855	26.379	47.180
	Present	7.8561	26.3839	47.1965

3	She et al. [17]	7.449	22.672	37.440
	Present	7.4490	22.6757	37.4526
4	She et al. [17]	6.972	19.399	30.384
	Present	6.9725	19.4024	30.3941
5	She et al. [17]	6.476	16.731	25.329
	Present	6.4760	16.7336	25.3376

Table 3 Comparisons of the nondimensional natural frequency for SS FG nanotube with various values of length-scale parameter l and using UTR

$l\ (nm)$		Ω_1	Ω_2	Ω_3
0	She et al. [17]	8.234	31.154	64.833
	Present	8.2346	31.1597	64.8547
1	She et al. [17]	8.335	32.655	71.671
	Present	8.3356	32.6611	71.6950
2	She et al. [17]	8.631	36.793	89.089
	Present	8.6314	36.7999	89.1195
3	She et al. [17]	9.103	42.810	112.267
	Present	9.1032	42.8178	112.3053
4	She et al. [17]	9.725	50.032	138.339
	Present	9.7252	50.0414	138.3863
5	She et al. [17]	10.470	58.012	165.947
	Present	10.4708	58.0223	166.0033

The results from Tables (2,3) presents validation of the present work. In addition to the nondimensional natural frequency, this paper also deals with the critical fluid velocity and thermal buckling load. The influence of thermal load and fluid velocity on the nondimensional natural frequency is also observed. The critical dimensionless fluid velocity is observed in this investigation, and results are presented in Table 4. It should be noted that linear temperature rise (LTR) is used, but also length-scale parameter is not neglected. As it can be seen, increasing nonlocal parameter μ leads to decrease in the critical fluid velocity. A decrease in the critical fluid velocity was observed with an increasing temperature change.

Results of the nondimensional natural frequency can be seen through Table 5. It can be observed how increasing the dimensionless fluid velocity has impacted the nondimensional natural frequency. Also, results are presented for different beam theory, that can be done by setting function $g(y,z)=0$ and $g(y,z)=z$, which corresponds to Euler-Bernoulli and Timoshenko beam theory, respectively, while refined beam theory is defined above.

Table 4 Dimensionless critical fluid velocity v_{cr} for different values of thermal load ($p=1$, $l=1$, $L/R_o=20$, LTR)

$\mu\,[nm]$	$\Delta T\,[K]$			
	0	100	200	300
0	14.2966	13.6522	12.9407	12.1513
1	14.1223	13.4719	12.7529	11.9537
2	13.6348	12.9667	12.2251	11.3965
3	12.9229	12.2259	11.4469	10.5689
4	12.0892	11.3531	10.5222	9.5736
5	11.2198	10.4351	9.5381	8.4953

Table 5 Nondimensional natural frequency Ω_1 for different values of dimensionless fluid velocity ($p=1$, $l=1$, $L/R_o=20$, $\Delta T=100$, LTR)

$\mu\,[nm]$	v					
	0			6		
	EBT	TBT	RBT	EBT	TBT	RBT
0	7.8203	7.7359	7.5936	7.0555	6.9617	6.8953
1	7.7173	7.6339	7.4911	6.9412	6.8481	6.7823
2	7.4289	7.3480	7.2038	6.6190	6.5279	6.4635
3	7.0059	6.9288	6.7819	6.1405	6.0522	5.9897
4	6.5077	6.4350	6.2838	5.5654	5.4799	5.4193
5	5.9839	5.9157	5.7587	4.9427	4.8596	4.8006

Impact of the nonlocal parameter on the critical fluid velocity is illustrated in Fig. (2). An increase in the nonlocal parameter has a pronounced reducing effect on the critical fluid velocity, especially for the higher values of the nonlocal parameter. Fig. (3) presents variation of the dimensionless critical fluid velocity for different values of the scale parameter ratio l/μ, as mentioned in She et al. [17]. For the case of dimensionless critical fluid velocity, for the value of the ratio $l/\mu=1$, the results are equal to the results for the classical continuum theory. The results can be obtained after neglecting the nonlocal and length-scale parameters. In the case when $l/\mu<1$, the critical fluid velocity has lower values than in the previous comparison. It can be noted from Table (4) that higher values of the nonlocal parameter led to lower values of the critical fluid velocity. In the case when $l/\mu>1$, the critical fluid velocity has higher values.

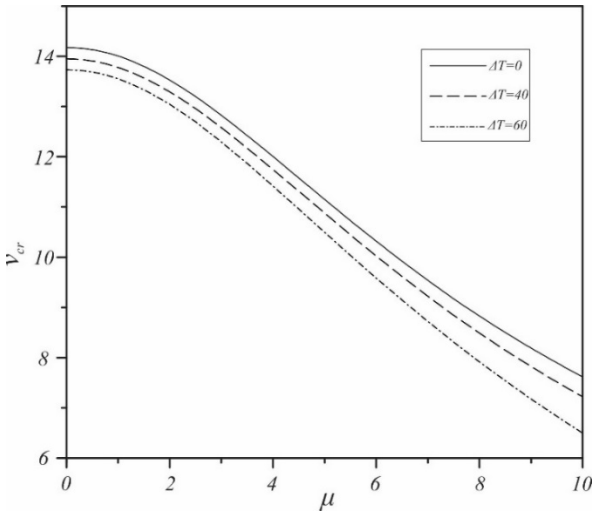

Fig. 2 Dimensionless critical fluid velocity versus nonlocal parameter with different values of thermal load ($p=1$, $l=0$, $L/R_o=20$, UTR)

The vibrations of the nanotube, in the presence of a fluid in the nanotube, are part of this investigation. Fig. (4) illustrates the dependence of the fluid velocity on the first nondimensional natural frequency. As can be seen, increasing the nanofluid dimensionless velocity leads to decrease in the nondimensional natural frequency. It also should be noted that by setting dimensionless fluid velocity to zero, nondimensional natural frequency that is obtained presents natural frequency with immovable fluid inside the nanotube. Decreasing in the nondimensional frequency significantly increases when the dimensionless fluid velocity approaches the critical value. It can also be noted that the results are presented for three different temperature values, so it can be concluded that the frequency decreases with an increase in thermal load. It means that increasing of the temperature leads to a critical value which can be investigated. Based on that, Fig. (5) presents the impact of thermal load on the nondimensional natural frequency, where the nondimensional natural frequency decreases significantly in the critical thermal load zone.

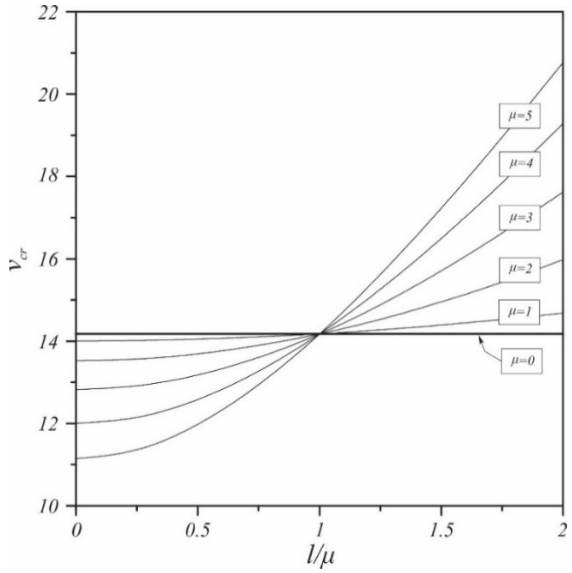

Fig. 3 Changes in dimensionless critical fluid velocity with different parameter ratios l/μ ($p=1$, $\Delta T=0$, $L/R_o=20$, UTR)

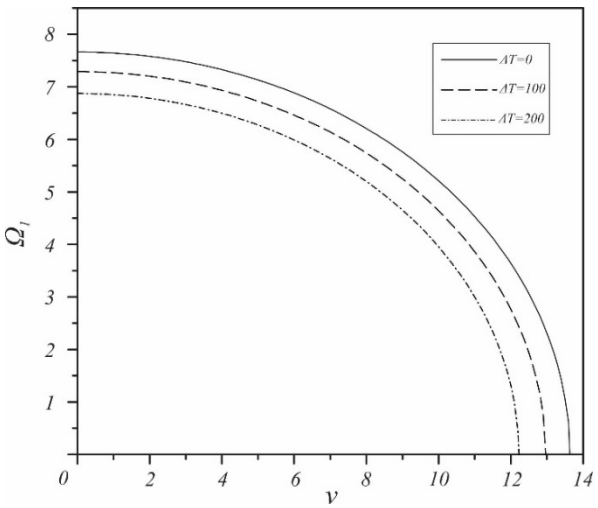

Fig. 4 Dependance of nondimensional natural frequency and fluid velocity with different values of the thermal load ($p=1$, $\mu=2$, $l=1$, $L/R_o=20$, LTR)

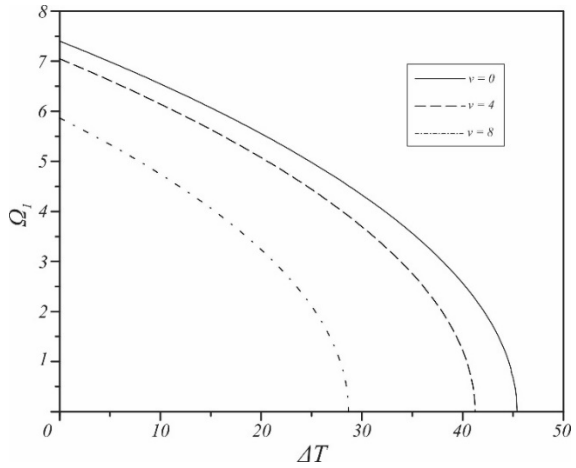

Fig. 5 Dependance of nondimensional natural frequency and the thermal load with different values of fluid velocity ($p=1$, $\mu=2$, $l=1$, $L/R_o=100$, LTR)

Temperature increase leads to decrease of the nondimensional natural frequency, which was obtained and considered. As it is mentioned above, increasing of temperature leads to critical buckling value at some point which can be seen in Fig. (5).

5. CONCLUSION

In this paper, investigation of the vibrations, critical fluid flow velocity and critical thermal load of the fluid-conveying FG nanotube model is presented. The equations of motion were obtained by using Hamilton's principle and based on the higher order refined beam theory within the framework of the nonlocal strain gradient theory. The results of the mentioned problem were obtained by using Galerkin's method, and the influence of the nonlocal and strain gradient parameters on the nondimensional frequencies and critical fluid velocity were presented. As it is mentioned above, the material of the nanotube was defined with power-law rule of mixture. It can be concluded that the nonlocal parameter and length-scale parameter have a significant impact on the nondimensional natural frequency and dimensionless fluid velocity, which was presented in the above tables and graphs. Also, the existence of the fluid in the nanotube leads to decrease of the natural frequency. A decrease of the natural frequency is more significant with the increasing fluid velocity. The impact of the thermal load on the nondimensional natural frequency was also considered. The conclusion of this part is like the influence of the fluid velocity, an increase of the thermal load leads to decrease of the natural frequency.

REFERENCES

1. Zhu, J., Lai, Z., Yin, Z., Jeon, J., Lee, S., 2001, *Fabrication of ZrO_2/AISI316L functionally graded materials for joint prostheses*, Materials Chemistry and Pshysics, 68, pp. 130-135.

2. Mishina, H., Inumaru, Y., Kaitoku, K., 2008, *Fabrication of ZrO_2-NiCr functionally graded material by powder metallurgy*, Materials Science and Engineering A, 475, pp. 141-147.
3. Kurimoto, M., Kato, K., Hanai, M., Hoshina, Y., Takei, M., Okubo H., 2010, *Application of functionally graded material for reducing electric field on electrode and spacer interface*, IEEE Tranasactions on Dieletrics and Electrical Insulation, 17(1), pp. 256-263.
4. Kato, K., Kurimoto, M., Shumiya, H., Adachi, H., Sakuma, S., Okubo H., 2010, *Application of functionally graded material for solid insulator in gaseous insulation system*, IEEE Tranasactions on Dieletrics and Electrical Insulation, 13(2), pp. 362-372.
5. Eringen, A. C., 1983, *On differential equations on nonlocal elasticity and solutions of screw dislocation and surface waves*, Journal of Applied Physics, 54, pp. 4703-4710.
6. Eringen, A. C., 2002, *Nonlocal continuum field theories*, Springer Science & Business Media, New York.
7. Eltaher, M. A., Emam, S. A., Mahmoud, F. F., 2013, *Static and stability analysis of nonlocal functionally graded nanobeams*, Composite Structures, 96, pp. 82-88.
8. Eltaher, M. A., Emam, S. A., Mahmoud, F. F., 2012, *Free vibration analysis of functionally graded size-dependent nanobeams*, Applied Mathematics and Computation, 218, pp. 7406-7420.
9. Ebrahimi, F., Salari, E., 2015, *Nonlocal thermo-mechanical vibration analysis of functionally graded nanobeams in thermal environment*, Acta Astronautica, 113, pp. 29-50.
10. Ebrahimi, F., Salari, E., 2015, *Thermal buckling and free vibration analysis of size dependent Timoshenko FG nanobeams in thermal environments*, Composite Structures, 128, pp. 363-380.
11. Jouneghani, F. Z., Dimitri, R., Tornabene, F., 2018, *Structural response of porous FG nanobeams under hygro-thermo-mechanical loadings*, Composites Part B, 152, pp. 71-78.
12. Ebrahimi, F, Barati, M. R., 2017, *Hygrothermal effects on vibration characteristics of viscoelastic FG nanobeams based on nonlocal strain gradient theory*, Composite Structures, 159, pp. 433-444.
13. Simsek, M., 2019, *Some closed-form solutions for static, buckling, free and forced vibration of functionally graded (FG) nanobeams using nonlocal strain gradient theory,* Composite Structures, 224, pp. 111041.
14. Lim, C., W., Zhang, G., Reddy, J., N., 2015, *A higher-order nonlocal elasticity and strain gradient theory and its applications in wave propagation,* Journal of the Mechanics and Physics of Solids, 78, pp. 298-313.
15. Janevski, G., Despenić, N., Pavlović, I., 2020, *Thermal buckling and free vibration of Euler-Bernoulli FG nanobeams on the higher-order nonlocal strain gradient theory,* Archives of Mechanics, 72, pp. 139-167.
16. Janevski, G., Pavlović, I., Despenić, N., 2020, *Thermal buckling and free vibration of Timoshenko FG nanobeams on the higher-order nonlocal strain gradient theory,* Journal of Mechanics of Materials and Structures, 15, pp. 107-133.
17. Nematollahi, M. S., Mohammadi, H., 2019, *Geometrically nonlinear vibration analysis of sandwich nanoplates based on higher-order nonlocal strain gradient theory,* International Journal of Mechanical Science, 156, pp. 31-45.
18. She, G. L., Yuan, F. G., Ren, Y. R., Xiao, W. S., 2017, *On buckling and postbuckling behavior of nanotubes,* International Journal of Engineering Science, 121, pp. 130-142.
19. She, G. L., Yuan, F. G., Ren, Y. R., Xiao, W. S., 2018, *On vibration of porous nanotubes,* International Journal of Engineering Science, 125, pp. 23-35.
20. She, G. L., Yuan, F. G., Ren, Y. R., 2018, *On wave propagation of porous nanotubes,* International Journal of Engineering Science, 130, pp. 62-74.
21. Shafiei, N., She, G. L., 2017, *On vibration of functionally graded nano-tubes in the thermal environment,* International Journal of Engineering Science, 133, pp. 84-98.
22. Lu, L., She, G. L., Xingming, G., 2021, *Size-dependent postbuckling analysis of graphene reinforced composite microtubes with geometrical imperfection,* International Journal of Mechanical Science, 199, pp. 106428.
23. Karami, B., Janghorban, M., 2019, *On the dynamics of porous nanotubes with variable material properties and variable thickness,* International Journal of Engineering Science, 136, pp. 53-66.
24. Wang, L., 2010, *Vibration analysis of fluid-conveying nanotubes with consideration of surface effects,* Physica E, 43, pp. 437-439.
25. Seyranian, A. P., Mailybaev, A. A., 2003, *Multiparameter stability theory with mechanical applications,* Vol. 13, World Scientific.
26. Deng, J., Liu, Y., Zhang, Z., Liu, W., 2017, *Size-dependent vibration and stability of multi-span viscoelastic functionally graded material nanopipes conveying fluid using a hybrid method,* Composite Structures, 179, pp. 590-600.
27. Liu, H., Zhang, L., Tang, H., 2019, *Nonlinear vibration and instability of functionally graded nanopipes with initial imperfection conveying fluid,* Applied Mathematical Modelling, 76, pp. 133-150.
28. Farajpour, A., Farokhi, H., Ghayesh, M. H., Hussain, S., 2018, *Nonlinear mechanics of nanotubes conveying fluid,* International Journal of Engineering Science, 133, pp. 132-143.

29. Hosseini, S. H. S., Ghadiri, M., 2021, *Nonlinear dynamics of fluid conveying double-walled nanotubes incorporating surface effect: A bifurcation analysis,* Applied Mathematical Modelling, 92, pp. 594-611.
30. Bahaadini, R., Hosseini, M., 2016, *Nonlocal divergence and flutter instability analysis of embedded fluid-conveying carbon nanotube uder magnetic field,* Microfluidics and Nanofluidics, 20, pp. 1-14.
31. Ghane, M., Saidi, A. R., Bahaadini, R., 2020, *Vibration of fluid-conveying nanotubes subjected to magnetic field based on the thin-walled Timoshenko beam theory,* Applied Mathematical Modelling, 80, pp. 65-83.
32. Nematollahi, M. A., Jamali, B., Hosseini, M., 2019, *Fluid velocity and mass ratio identification of piezoelectric nanotube conveying fluid using inverse analysis,* Acta Mechanica, 231, pp. 683-700.
33. Simsek, M., Yurtcu, H. H., 2013, *Analytical solutions for bending and buckling of functionally graded nanobeams based on the nonlocal Timoshenko beam theory,* Composite Structures, 97, pp. 378-386.
34. Touloukian, T. S., 1967, *Thermophysical Properties of High Temperature Solid Materials,* 1, Elements, Macmillan New York.
35. Zhang P., Fu, Y., 2013, *A higher-order beam model for tubes,* European Journal of Mechanics A/Solids, 38, pp. 12-19.